Vol 11 No 5, May 2002
1009-1963/2002/11(05)/0461-06
Chinese Physics
© 2002 Chin. Phys. Soc.
and IOP Publishing Ltd

A special form of electrodynamical response to a gravitational wave: outgoing and imploding photon fluxes*

Li Fang-Yu (李芳昱)[a], Su Xun(苏 荀)[a],
Long Bing-Wei(龙炳蔚)[a], and Tang Meng-Xi(唐孟希)[b]

[a] *Department of Physics, Chongqing University, Chongqing 400044, China*

[b] *Department of Physics, Zhongshan University, Guangzhou 510275, China*

(Received 10 April 2001; revised manuscript received 6 January 2002)

We have investigated the interaction of an electromagnetic (EM) wave with a standing gravitational wave (GW) in an external static magnetic field, and obtained concrete forms of first-order perturbative EM energy fluxes. Unlike the propagating properties of the "left-circular" and "right-circular" waves of the tangential perturbative energy fluxes around the symmetrical axis, the radial perturbative energy fluxes are expressed as the outgoing and imploding waves to the symmetrical axis. We also examine several physical examples and show that this effect can produce very small but nonvanishing radial perturbative photon fluxes. This may be useful for EM detection of the high-frequency relic GWs of the GHz region in quintessential inflationary models.

Keywords: gravitational wave, electrodynamical response, outgoing and imploding photon fluxes
PACC: 0440, 0480, 0430

1. Introduction

Though the electromagnetic (EM) detection and generation of the gravitational waves (GWs) in laboratory conditions have been extensively discussed,[1−6] the Grishchuk–Sazhin (G–S) model[5,6] and the composite toroidal EM resonant system[7] may be the most typical schemes, because they represent the ultimate form that one can hope to achieve in terms of compactness, geometric efficiency and energy storage. Thus they have aroused extensive interest and reviews.[1,2,8−10] Large gaps between the schemes and reality are mainly expressed as the excessive signal accumulation time ($\sim 10^5$s), giant dimensions ($\sim 10^2-10^4$m^3) of the whole system, and power losses ($\sim 10^7-10^8$W).[5−7]

In some previous works[11,12] we considered a new scheme, in which we showed that, if the detecting system is not an EM cavity but an EM wave propagating along the symmetrical axis z of the focal region of the G–S toroidal EM cavity, where a static magnetic field is distributed within the focal region, then under special resonant conditions it is possible to provide a new way of simultaneously narrowing such gaps, as stated above. Namely, in this case not only the first-order axial perturbative EM energy fluxes can be generated, but the tangential perturbative energy fluxes can also be produced. The latter are perpendicular to the propagating direction of the background EM wave. Thus, this effect might provide a new possibility to resolve and display the EM perturbation caused by the GW.

In fact, in addition to the tangential perturbation, there is the radial perturbation. Although the tangential and radial perturbative energy fluxes have much in common, there are some important differences. As shown below, the major properties of the radial perturbative energy fluxes are expressed as the outgoing and imploding waves in the local regions, or in quantum language, as the outgoing and imploding photon fluxes. Moreover, the maximum of the radial perturbative energy flux is almost one order of magnitude greater than that of the tangential perturbative energy flux. In particular, the resonant frequency discussed in this paper is just distributed in the peak value region of the high-frequency relic GWs, expected by quintessential inflationary models.[13] Therefore, such properties may be very useful for further improving the electrodynamical response of the GWs and detecting the relic GWs in the GHz frequency window.

*Project supported by the National Natural Science Foundation of China (Grant Nos 10175096 and 19835040).

2. Construction of the energy-momentum tensor of the EM fields in the GW field

The time-dependent perturbation solutions we obtained in Ref.[11] for the Maxwell equations in a curved space-time caused by the standing GW are given by (in MKS units)

$$\begin{aligned}
E_{\phi}^{(1)} =&\frac{1}{2}AcB_z^{(0)}k_{\rm g}r{\rm J}_1(k_{\rm g}r)\sin(\omega_{\rm g}t+\delta),\\
B_z^{(1)} =&AB_z^{(0)}\left[{\rm J}_0(k_{\rm g}r)-\frac{1}{2}k_{\rm g}r{\rm J}_1(k_{\rm g}r)\right]\cos(\omega_{\rm g}t+\delta),\\
E_r^{(1)} =&E_z^{(1)}=B_r^{(1)}=B_{\phi}^{(1)}=0,
\end{aligned}\tag{1}$$

$$\begin{aligned}
\tilde{E}_r^{(1)} =&A_1(r)\cos\phi{\rm Re}[\exp\{{\rm i}[(\omega_{\rm g}+\omega_{\rm e})t-k_{\rm e}z+\delta]\}]\\
&+A_2(r)\cos\phi{\rm Re}[\exp\{{\rm i}[(\omega_{\rm g}-\omega_{\rm e})t+k_{\rm e}z+\delta]\}],\\
\tilde{E}_{\phi}^{(1)} =&B_1(r)\sin\phi{\rm Re}[\exp\{{\rm i}[(\omega_{\rm g}+\omega_{\rm e})t-k_{\rm e}z+\delta]\}]\\
&+B_2(r)\sin\phi{\rm Re}[\exp\{{\rm i}[(\omega_{\rm g}-\omega_{\rm e})t+k_{\rm e}z+\delta]\}],\\
\tilde{E}_z^{(1)} =&C_1(r)\cos\phi{\rm Im}[\exp\{{\rm i}[(\omega_{\rm g}+\omega_{\rm e})t-k_{\rm e}z+\delta]\}]\\
&+C_2(r)\cos\phi{\rm Im}[\exp\{{\rm i}[(\omega_{\rm g}-\omega_{\rm e})t+k_{\rm e}z+\delta]\}],\\
\tilde{B}_r^{(1)} =&\frac{D_1(r)}{c}\sin\phi{\rm Re}[\exp\{{\rm i}[(\omega_{\rm g}+\omega_{\rm e})t-k_{\rm e}z+\delta]\}]\\
&+\frac{D_2(r)}{c}\sin\phi{\rm Re}[\exp\{{\rm i}[(\omega_{\rm g}-\omega_{\rm e})t+k_{\rm e}z+\delta]\}],\\
\tilde{B}_{\phi}^{(1)} =&\frac{F_1(r)}{c}\cos\phi{\rm Re}[\exp\{{\rm i}[(\omega_{\rm g}+\omega_{\rm e})t-k_{\rm e}z+\delta]\}]\\
&+\frac{F_2(r)}{c}\cos\phi{\rm Re}[\exp\{{\rm i}[(\omega_{\rm g}-\omega_{\rm e})t+k_{\rm e}z+\delta]\}],\\
\tilde{B}_z^{(1)} =&\frac{G_1(r)}{c}\sin\phi{\rm Im}[\exp\{{\rm i}[(\omega_{\rm g}+\omega_{\rm e})t-k_{\rm e}z+\delta]\}]\\
&+\frac{G_2(r)}{c}\sin\phi{\rm Im}[\exp\{{\rm i}[(\omega_{\rm g}-\omega_{\rm e})t+k_{\rm e}z+\delta]\}],
\end{aligned}\tag{2}$$

where Eqs.(1) and (2) represent the first-order perturbation produced by the direct interaction of the standing GW with the static magnetic field and the EM wave, respectively (i.e. $F_{\mu\nu}^{(1)}$ and $\tilde{F}_{\mu\nu}^{(1)}$ are the first-order perturbations to the background EM tensor $F_{\mu\nu}^{(0)}$ in the presence of the GW), A is the amplitude of the standing GW, ${\rm J}_0$ and ${\rm J}_1$ are Bessel functions, $\omega_{\rm g}$ and $k_{\rm g}$ are, respectively, the angular frequency and wave vector of the GW, $B_z^{(0)}$ is the external static magnetic field, δ is a retarded phase factor. A_1 A_2 ... G_1 G_2 in Eq.(2) are functions of $r, k_{\rm e}$ and $k_{\rm g}$, their specific forms are given in Ref.[11].

Now we can construct the energy-momentum tensor (EMT) of the EM fields in the GW. According to generic expression for the EMT of the EM fields

$$T^{\mu\nu}=\frac{1}{\mu_0}\left(-F^{\mu}{}_{\alpha}F^{\nu\alpha}+\frac{1}{4}g^{\mu\nu}F_{\alpha\beta}F^{\alpha\beta}\right),\tag{3}$$

and with the help of Eqs.(1) and (2), and using the form of the standing GW in the synchronous gauge reference (and using standard cylindrical polar coordinates expressions)[5,7,11]

$$\begin{aligned}
h_{11} =&h_{rr}=-A\frac{{\rm J}_1(k_{\rm g}r)}{k_{\rm g}r}\cos(\omega_{\rm g}t+\delta),\\
h_{22} =&h_{\varphi\varphi}=-Ar^2\left[{\rm J}_0(k_{\rm g}r)-\frac{{\rm J}_1(k_{\rm g}r)}{k_{\rm g}r}\right]\cos(\omega_{\rm g}t+\delta),\\
h_{33} =&h_{zz}=A{\rm J}_0(k_{\rm g}r)\cos(\omega_{\rm g}t+\delta),
\end{aligned}\tag{4}$$

we obtain

$$\begin{aligned}
{}^{(0)}T^{00} =&\varepsilon_0[(E_r^{(0)})^2+(E_{\varphi}^{(0)})^2]\\
&+\frac{1}{\mu_0}[(B_r^{(0)})^2+(B_{\varphi}^{(0)})^2+(B_z^{(0)})^2],
\end{aligned}\tag{5}$$

$$\begin{aligned}
{}^{(1)}T^{00} =&\varepsilon_0\left[E_r^{(0)}\tilde{E}_r^{(1)}+E_{\varphi}^{(0)}(E_{\varphi}^{(1)}+\tilde{E}_{\varphi}^{(1)})\right.\\
&\left.+\frac{1}{2}h_{rr}(E_r^{(0)})^2+\frac{1}{2}\frac{h_{\varphi\varphi}}{r^2}(E_{\varphi}^{(0)})^2\right]\\
&+\frac{1}{\mu_0}\left[B_r^{(0)}\tilde{B}_r^{(1)}+B_{\varphi}^{(0)}\tilde{B}_{\varphi}^{(1)}\right.\\
&+B_z^{(0)}(B_z^{(1)}+\tilde{B}_z^{(1)})+\frac{1}{2}\left(h_{zz}+\frac{h_{\varphi\varphi}}{r^2}\right)(B_r^{(0)})^2\\
&+\frac{1}{2}(h_{rr}+h_{zz})(B_{\varphi}^{(0)})^2\\
&\left.+\frac{1}{2}\left(h_{rr}+\frac{h_{\varphi\varphi}}{r^2}\right)(B_z^{(0)})^2\right],
\end{aligned}\tag{6}$$

$$\begin{aligned}
{}^{(2)}T^{00} =&\varepsilon_0\left[(E_r^{(1)})^2+(E_{\varphi}^{(1)}+\tilde{E}_{\varphi}^{(1)})^2+(E_z^{(1)})^2\right.\\
&\left.+h_{rr}E_r^{(0)}\tilde{E}_r^{(1)}+\frac{h_{\varphi\varphi}}{r^2}E_{\varphi}^{(0)}(E_{\varphi}^{(1)}+\tilde{E}_{\varphi}^{(1)})\right]\\
&+\frac{1}{\mu_0}\left[(\tilde{B}_r^{(1)})^2+(\tilde{B}_{\varphi}^{(1)})^2+(B_z^{(1)}+\tilde{B}_z^{(1)})^2\right.\\
&+\left(h_{zz}+\frac{h_{\varphi\varphi}}{r^2}\right)B_r^{(0)}\tilde{B}_r^{(1)}+(h_{rr}+h_{zz})B_{\varphi}^{(0)}\tilde{B}_{\varphi}^{(1)}\\
&\left.+\left(h_{rr}+\frac{h_{\varphi\varphi}}{r^2}\right)B_z^{(0)}(B_z^{(1)}+\tilde{B}_z^{(1)})\right]\approx O(h^2),
\end{aligned}\tag{7}$$

$$\begin{aligned}
{}^{(0)}S^z=c\ {}^{(0)}T^{03} =&\frac{1}{\mu_0}(E_r^{(0)}E_{\varphi}^{(0)}-E_{\varphi}^{(0)}B_r^{(0)})\\
=&\frac{1}{\mu_0}E_x^{(0)}B_y^{(0)},
\end{aligned}\tag{8}$$

$$\begin{aligned}
{}^{(1)}S^r =c\ {}^{(1)}T^{01} =&\frac{1}{\mu_0}(E_{\varphi}^{(0)}B_z^{(1)}+E_{\varphi}^{(0)}\tilde{B}_z^{(1)}\\
&-\tilde{E}_z^{(1)}B_{\varphi}^{(0)}+E_{\varphi}^{(1)}B_z^{(0)}+\tilde{E}_{\varphi}^{(1)}B_z^{(0)}),
\end{aligned}\tag{9}$$

$$\overset{(1)}{S}{}^{\varphi} = c\ \overset{(1)}{T}{}^{02} = \frac{1}{\mu_0}(\tilde{E}_z^{(1)} B_r^{(0)} - E_r^{(0)} B_z^{(1)} - E_r^{(0)} \tilde{B}_z^{(1)} - \tilde{E}_r^{(1)} B_z^{(0)}), \quad (10)$$

$$\overset{(1)}{S}{}^{z} = c\ \overset{(1)}{T}{}^{03} = \frac{1}{\mu_0}(E_r^{(0)} \tilde{B}_\varphi^{(1)} + \tilde{E}_r^{(1)} B_\varphi^{(0)} - E_\varphi^{(0)} \tilde{B}_r^{(1)} + E_\varphi^{(1)} B_r^{(0)} + \tilde{E}_\varphi^{(1)} B_r^{(0)}), \quad (11)$$

$$\begin{aligned} \overset{(2)}{S}{}^{r} &= c\ \overset{(2)}{T}{}^{01} \approx O(h^2), \\ \overset{(2)}{S}{}^{\phi} &= c\ \overset{(2)}{T}{}^{02} \approx O(h^2), \\ \overset{(2)}{S}{}^{z} &= c\ \overset{(2)}{T}{}^{03} \approx O(h^2). \end{aligned} \quad (12)$$

Because the EM field tensors satisfy $|F_{\mu\nu}^{(1)}|$, $|\tilde{F}_{\mu\nu}^{(1)}| \ll |F_{\mu\nu}^{(0)}|$ for the nonvanishing $F_{\mu\nu}^{(0)}$, $F_{\mu\nu}^{(1)}$ and $\tilde{F}_{\mu\nu}^{(1)}$, we have $|\overset{(0)}{T}{}^{\mu\nu}| \gg |\overset{(1)}{T}{}^{\mu\nu}| \gg |\overset{(2)}{T}{}^{\mu\nu}|$ for the nonzero $\overset{(0)}{T}{}^{\mu\nu}$, $\overset{(1)}{T}{}^{\mu\nu}$ and $\overset{(2)}{T}{}^{\mu\nu}$, where $\overset{(0)}{T}{}^{\mu\nu}$ is the EMT of the background EM fields, while $\overset{(1)}{T}{}^{\mu\nu}$ and $\overset{(2)}{T}{}^{\mu\nu}$ represent the first-order and second-order perturbations to $\overset{(0)}{T}{}^{\mu\nu}$ in the presence of the GW, respectively. Consequently, for the effect of the GW, we are interested in $\overset{(1)}{T}{}^{\mu\nu}$ but not in $\overset{(0)}{T}{}^{\mu\nu}$ and $\overset{(2)}{T}{}^{\mu\nu}$. Nevertheless, it is easily shown from Eq.(7), that the average value of $\overset{(2)}{T}{}^{00}$ with respect to time is always positive. Thus it expresses essentially the net increasing quantity of the energy density of the EM fields. Especially, under resonant conditions, it should correspond to the resonant graviton–photon conversion at a quantum level.[2,10] Unfortunately, even under limit conditions of the present experimental possibilities, the second-order perturbation is still far below the requirements of the observable effect.[9,10] Therefore, it has only theoretical interest. But for some astrophysical situations, an observable effect is possible because very large EM fields and very strong GWs often occur simultaneously.[14]

3. The radial perturbation: the outgoing and imploding photon fluxes

In the following, we study mainly the first-order radial perturbative energy fluxes. Equations (9)–(11) (i.e. $\overset{(1)}{S}{}^{r}$, $\overset{(1)}{S}{}^{\varphi}$ and $\overset{(1)}{S}{}^{z}$) represent the first-order radial, tangential and axial perturbative energy fluxes, respectively. For high-frequency perturbative energy fluxes (here we discuss the perturbative effects at frequency of $\nu \sim 10^9$Hz), only their nonvanishing average values with respect to time have an observable effect. It is easily seen from Eqs.(1), (2), (9)–(11), that the average values of the perturbative energy fluxes, Eqs.(9)–(11) vanish in the whole frequency ranges of $\omega_e \neq \omega_g$ and $\omega_e \neq \omega_g/2$. In other words, only under the condition of $\omega_e = \omega_g/2$ (half-frequency resonance) or $\omega_e = \omega_g$ (synchroresonance), $\overset{(1)}{S}{}^{r}$, $\overset{(1)}{S}{}^{\varphi}$ and $\overset{(1)}{S}{}^{z}$ have nonvanishing average values with respect to time. In the following, we study only the radial perturbative energy flux $<\overset{(1)}{S}{}^{r}>$. Here the symbol $<\ >$ means the average value with respect to time.

Introducing Eqs.(1) and (2) (including concrete expressions of the amplitudes of $\tilde{B}_z^{(1)}$ and $\tilde{E}_z^{(1)}$ presented in Ref.[11]) into Eqs.(9), and setting $\delta = \pi$ (which is always possible), $\omega_e = \omega_g/2$ and $\omega_e = \omega_g$, we have

$$<\overset{(1)}{S}{}^{r}>_{\omega_e=\frac{\omega_g}{2}} = \frac{1}{\mu_0} < E_\varphi^{(0)} \tilde{B}_z^{(1)} - \tilde{E}_z^{(1)} B_\varphi^{(0)} >_{\omega_e=\frac{\omega_g}{2}} = \frac{Aa^2}{4\mu_0 c}[f_1(r)\sin^2\varphi + f_2(r)\cos^2\varphi]\sin(k_g z), \quad (13)$$

where

$$f_1(r) = \sum_{p=0}^{\infty}(-1)^p \left\{ \frac{(2p^2+8p+7)k_e^{2p+3} r^{2p+3}}{[(2p+4)^2-4](p+1)!(p+2)!} - \frac{k_e^{2p+1} r^{2p+1}}{4(p+1)!(p+2)!} \right\}, \quad (14)$$

$$f_2(r) = \sum_{p=0}^{\infty}(-1)^p \left\{ \frac{2(p+3)k_e^{2p+3} r^{2p+3}}{[(2p+3)^2-1]p!(p+2)!} \right\}, \quad (15)$$

and

$$<\overset{(1)}{S}{}^{r}>_{\omega_e=\omega_g} = \frac{1}{\mu_0} < E_\varphi^{(0)} B_z^{(1)} >_{\omega_e=\omega_g} = \frac{Aa^2 B_z^{(0)}}{\mu_0}[2\mathrm{J}_0(k_g r) - k_g r \mathrm{J}_1(k_g r)] \times \sin\varphi\cos(k_g z). \quad (16)$$

Equations (13) and (16) express the average values of $\overset{(1)}{S}{}^{r}$ with respect to time under the resonant conditions of $\omega_e = \omega_g/2$ (half-frequency resonance) and $\omega_e = \omega_g$ (synchroresonance).

Figures 1 and 2 give the rating curves between the functions $f_1(r)$, $f_2(r)$ and the radial coordinate r; and the relative parameters are chosen to be $\lambda_e = 2\lambda_g$=0.2m. Figure 3 gives the angular distribution of $<\overset{(1)}{S}{}^{r}>_{\omega_e=\omega_g/2}$ at the plane $z = \lambda_g/4$.

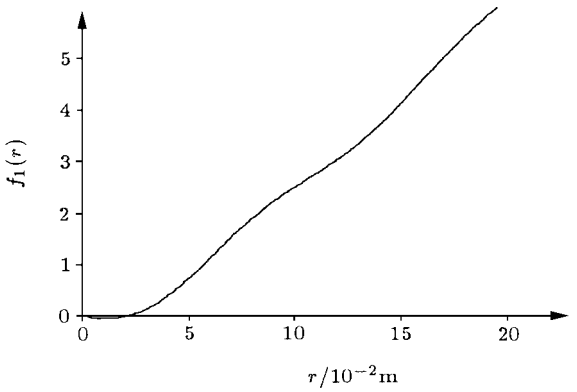


Fig.1. Rating curve between the function $f_1(r)$, Eq.(14), and the radial coordinate r. Here $\lambda_e = 2\lambda_g$=0.2m.

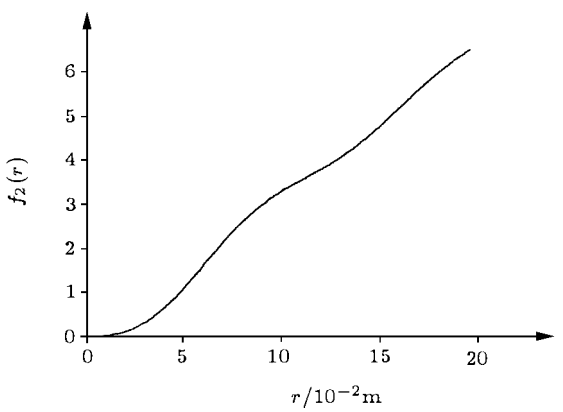


Fig.2. Rating curve between the function $f_2(r)$, Eq.(15), and the radial coordinate r. Here $\lambda_e = 2\lambda_g$=0.2m.

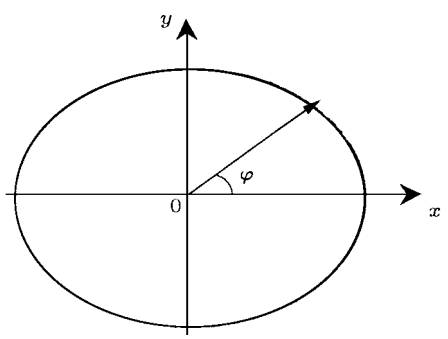


Fig.3. Angular distribution of $<\overset{(1)}{S^r}>_{\omega_e=\omega_g/2}$ at the circumference of $r = \lambda_e = 2\lambda_g$=0.2m and the plane $z = \lambda_g/4$.

It is easy to show that $<\overset{(1)}{S^r}>_{\omega_e=\omega_g/2}$ has a similar distribution at the plane $z = -\lambda_g/4$, but the propagating directions are contrary to that at the plane $z = \lambda_g/4$.

Figure 4 gives the angular distribution of $<\overset{(1)}{S^r}>_{\omega_e=\omega_g}$ at the plane z=0. It is also easy to show that $<\overset{(1)}{S^r}>_{\omega_e=\omega_g}$ has a similar distribution at the plane $z = \lambda_g/2$, but the propagating directions are contrary to that at the plane z=0.

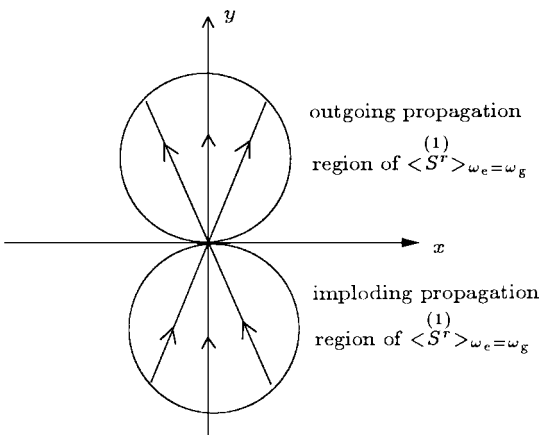


Fig.4. Angular distribution of $<\overset{(1)}{S^r}>_{\omega_e=\omega_g}$ at the circumference of $r = \lambda_e = \lambda_g$=0.1m and the plane z=0.

Equations (13)–(15), Figs.1–3 and the angular distribution of $<\overset{(1)}{S^r}>_{\omega_e=\omega_g/2}$ show that $<\overset{(1)}{S^r}>_{\omega_e=\omega_g/2}$ is expressed as the outgoing perturbative energy flux at the plane $z = \lambda_g/4$, but as the imploding perturbative energy flux at the plane $z = -\lambda_g/4$, and their maximums occur at $\varphi = 0, \pi$. In the above two cases, the angular distributions of $<\overset{(1)}{S^r}>_{\omega_e=\omega_g/2}$ are all ellipses. Equation (16) and Fig.4 show that $<\overset{(1)}{S^r}>_{\omega_e=\omega_g}$ at the plane z=0, has maximums at $\varphi = \pm\pi/2$, while it vanishes at $\varphi = 0, \pi$. In the region of $0 < \varphi < \pi$, $<\overset{(1)}{S^r}>_{\omega_e=\omega_g}$ is expressed as the outgoing perturbative energy flux, while in the region of $\pi < \varphi < 2\pi$, it is expressed as the imploding perturbative energy flux.

Integration of Eq.(16) over the cylinder ($r = R_c$=const., $-\lambda_g/4 \le z \le \lambda_g/4$, $0 \le \varphi \le \pi$ or $\pi \le \varphi \le 2\pi$) gives the total outgoing (or imploding) perturbative energy flux passing through the cylinder as follows

$$<\overset{(1)}{u^r}>_{\omega_e=\omega_g} = \int_{-\lambda_g/4}^{\lambda_g/4}\int_0^{\pi} <\overset{(1)}{S^r}>_{\omega_e=\omega_g, r=R_c} r\mathrm{d}\varphi\mathrm{d}z$$
$$= \frac{AaB_z^{(0)}R_c}{\mu_0 k_g}[2\mathrm{J}_0(k_gR_c) - k_gR_c\mathrm{J}_1(k_gR_c)]. \quad (17)$$

It can be shown from Eq.(17) that the first maximum of $<\overset{(1)}{u^r}>_{\omega_e=\omega_g}$ occurs at the position of $R_c \approx$

λ_g=0.1m. This means that the effective radially perturbative outgoing (or imploding) energy flux can be concentrated on the region with a magnitude of one wavelength λ_g near the axis. Equations (13) and (16) indicate that $<\overset{(1)}{S^r}>$ is often a function of the space coordinates r, φ, z, and there are corresponding "equivalent emission sources" and "equivalent imploding sources". Thus $\overset{(1)}{S^r}$ is essentially a radial energy flux (photon flux) fluctuation superimposed on the background EM fields in the local regions. In other words, the GW causes the change of the physical behaviour of the photons in the local regions.

It is interesting to compare the properties of the radial perturbative energy flux with those of the tangential one. In the same way, from Eq.(10), we can obtain the total tangential perturbative energy flux passing through the plane (φ=0, $0 \le r \le R_c$, $-\lambda_g/4 \le z \le \lambda_g/4$)[11]

$$<\overset{(1)}{u^\varphi}>_{\omega_e=\omega_g}=\frac{AaB_z^{(0)}}{2\mu_0 k_g}\int_0^{R_c}[2J_0(k_g r)-k_g r J_1(k_g r)]dr. \tag{18}$$

We have shown[11,12] that the effective tangentially perturbative energy flux can also be concentrated on the region with a magnitude of one wavelength λ_g near the axis. Consequently, we can compare the maximum of the radial perturbative energy flux with that of the tangential one in the same scale, although they have different propagating directions. From Eqs.(17) and (18), we have

$$\left[\frac{<\overset{(1)}{u^r}>_{\omega_e=\omega_g}}{<\overset{(1)}{u^\varphi}>_{\omega_e=\omega_g}}\right]_{R_c=\lambda_g=0.1m} = \left\{\frac{2R_c[2J_0(k_g R_c)-k_g R_c J_1(k_g R_c)]}{\int_0^{R_c}[2J_0(k_g r)-k_g r J_1(k_g r)]dr}\right\}_{R_c=\lambda_g=0.1m} \approx 10, \tag{19}$$

i.e. the effective radially perturbative energy flux is almost one order of magnitude higher than the effective tangentially perturbative energy flux. Thus, under the synchroresonance condition the radial perturbation has a better physical effect than the tangential perturbation. Nevertheless, due to the faintness of the interaction of the GW (gravitons) with the EM fields (photons), it is necessary to describe the perturbation in quantum language (photon flux). Clearly, the corresponding perturbative photon fluxes of $<\overset{(1)}{u^r}>_{\omega_e=\omega_g}$ and $<\overset{(1)}{u^\varphi}>_{\omega_e=\omega_g}$ can be written, respectively,

$$n_r=\frac{<\overset{(1)}{u^r}>_{\omega_e=\omega_g}}{\hbar\omega_e}, \tag{20}$$

$$n_\phi=\frac{<\overset{(1)}{u^\phi}>_{\omega_e=\omega_g}}{\hbar\omega_e}, \tag{21}$$

where $\hbar$ is the Planck constant. Therefore, the perturbative photon numbers caused by $<\overset{(1)}{u^r}>_{\omega_e=\omega_g}$ and $<\overset{(1)}{u^\varphi}>_{\omega_e=\omega_g}$ in the time interval Δt are

$$N_r=n_r\Delta t=\frac{AB_z^{(0)}a\Delta t}{\mu_0 k_g\hbar\omega_e} \times[2R_c J_0(k_g R_c)-k_g R_c^2 J_1(k_g R_c)], \tag{22}$$

$$N_\phi=n_\phi\Delta t=\frac{AB_z^{(0)}a\Delta t}{2\mu_0 k_g\hbar\omega_e}\int_0^{R_c}[2J_0(k_g r)-k_g r J_1(k_g r)]dr. \tag{23}$$

4. Numerical estimations

Now we choose some achievable limit values of the EM parameters for the present experiments. (1) $a=3\times10^5\mathrm{Vm}^{-1}$, $a/c=10^{-3}$T, the amplitude of the background EM wave. If the cross section of the background wave is limited in the region of radius $R_c=\lambda_e=\lambda_g$=0.1m, then the corresponding power is about 10^6W. This is equivalent to a photon flux $n^{(0)}$ of $10^{30}\mathrm{s}^{-1}$ roughly for the background EM wave of λ_e=0.1m. Modern klystrons or free-electron lasers can, in principle, generate such a power.[15] (2) $B_z^{(0)}$=30T, the strength of the background static magnetic field (this is the achievable strength of a stationary magnetic field under the present experimental condition[16]).

According to Eqs.(20)–(23) and the above parameters, and setting $\Delta t=10^3$s, we obtain the following results (see Table 1).

We see from Table 1 that, if $A=10^{-33}$, then $N_\phi=10^3$, $N_r=10^4$. Unfortunately, generating a standing GW with $A=10^{-33}$, λ_g=0.1m seems to be beyond the ability of the present experiments.[9,11,12] However, when $A=10^{-35}$, we have N_ϕ=10 and $N_r=10^2$. Although then the perturbative photon numbers are two orders of magnitude less than that of the first scheme, the requirements of other parameters can be greatly relaxed.[11,12] In particular, in this case the whole EM system can be reduced to the typical laboratory dimensions. It is worthwhile investigating further.

Table 1. The perturbative photon number N_r, N_ϕ and corresponding relevant parameters.

The tangential perturbation			The radial perturbation			A
$< \overset{(1)}{u^\phi} >_{\omega_e=\omega_g}$ /W	n_ϕ/s^{-1}	N_ϕ	$< \overset{(1)}{u^r} >_{\omega_e=\omega_g}$ /W	n_r/s^{-1}	N_r	
(a) 10^{-24}	1	10^3	10^{-23}	10	10^4	10^{-33}
(b) 10^{-25}	10^{-1}	10^2	10^{-24}	1	10^3	10^{-34}
(c) 10^{-26}	10^{-2}	10	10^{-25}	10^{-1}	10^2	10^{-35}

5. Concluding remarks

1. In this paper we have calculated the first-order radial perturbative photon fluxes produced by the high-frequency standing GW ($\nu \approx 10^9$Hz). Unlike the "left-circularly" and "right-circularly" propagating properties of the tangential perturbative photon fluxes, the radial perturbation is expressed as the outgoing and imploding photon fluxes around the symmetrical axis. Under the half-frequency resonance condition ($\omega_e = \omega_g/2$), we have $| < \overset{(1)}{S^r} >_{\omega_e=\omega_g/2} |_{r\to 0} \to 0$; while under the synchroresonance condition ($\omega_e = \omega_g$), the outgoing and imploding photon fluxes have the "anti-symmetry" around the symmetrical axis. Thus, in the above two cases there are no "accumulation" or "loss" effects of the photon fluxes at the symmetrical axis, i.e. there is no singular behaviour.

2. The effective tangentially and radially perturbative fluxes can all be concentrated on the region with a magnitude of one wavelength λ_g near the axis, but the maximum of the latter is one order of magnitude greater than that of the former. Since any photon measured in the local regions and in such special directions may be a signal of the EM perturbation produced by the GW, the scheme described in this paper provides a new possibility to resolve and improve the ER of the GW.

3. The energy spectra of the relic GWs, recently estimated by Giovannini[13] in the quintessential inflationary models, are expected to have quite a high spike region of the energy density in the GHz frequency window. It corresponds to a dimensionless amplitude of the order of 10^{-30}. This is about five orders of magnitude higher than that of the amplitude of the standing GW discussed here! Because our resonant frequency lies just in the peak value region, using this scheme (or other similar schemes of the small EM detectors[17]) for the detection purposes of the high-frequency relic GWs may be more useful.

For the purpose of ease and straightforwardness, our approach for the interaction of the EM fields with the GW is classical in itself. For quantum effects caused by the high-frequency relic GWs (gravitons) in the EM systems satisfying realizable boundary conditions, we will give further argument elsewhere.

References

[1] Cuomo D *et al* 1988 *Proc. Int. Symp. on Experimental Gravitational Physics* (Guangzhou China) ed by P F Michelson (Singapore: World Scientific) p262

[2] Long H N, Soa D V and Tuan T A 1994 *Phys. Lett.* A **186** 382

[3] Boccaletti D *et al* 1970 *Nuovo Cimento* B **70** 129

[4] Pinto I M and Rotoli G 1989 *8th Italian Conference on General Relativity and Gravitational Physics* ed by M G Gerdooio *et al* (Singapore: World Scientific) p560

[5] Grishchuk L P and Sazhin M V 1975 *Sov. Phys. JETP* **41** 787

[6] Grishchuk L P and Sazhin M V 1983 *Sov. Phys. JETP* **53** 1128

[7] Tang M X, Li F Y and Luo J 1997 *Acta Phys. Sin.* (*Overseas Edition*) **6** 161

[8] Tang M X and Li F Y 2000 *Class. Quantum Grav.* **17** 2449

[9] Gratta G *et al* 1992 *Workshop on Beam-Beam and Beam-Radiation Interaction: High Intensity and Nonlinear Effects* (Singapore: World Scientific) p70

[10] Logi W K and Mickelson A R 1977 *Phys. Rev.* D **16** 2915

[11] Li F Y *et al* 2000 *Phys. Rev.* D **62** 044018

[12] Li F Y, Tang M X and Wen D H 1999 *Chin. Phys. Lett.* **16** 12

[13] Giovannini M 1999 *Phys. Rev.* D **60** 123511

[14] Marklund M, Brodin G and Dunsby P 2000 *Astrophys. J.* **536** 875

[15] Chen P *et al* Ref.[9] p 84

[16] Boebinger G, Passner A and Bevk J 1995 *Sci. Am.* **272** 34

[17] Tang M X and Li F Y 1997 *Acta Phys. Sin.* **46** 238 (in Chinese)